Normal modes and discovery of high-order cross-frequencies in the DBV white dwarf GD 358

F. Vuille,[1][*][†] D. O'Donoghue,[2] D. A. H. Buckley,[2] C.-M. Massacand,[3][‡] J. E. Solheim,[3] S. Bard,[4] G. Vauclair,[5] O. Giovannini,[6][§] S. O. Kepler,[6] A. Kanaan,[7] J. L. Provencal,[8] M. A. Wood,[9] J. C. Clemens,[10] S. J. Kleinman,[11][¶] M. S. O'Brien,[12] R. E. Nather,[13] D. E. Winget,[13] A. Nitta,[13] E. W. Klumpe,[13] M. H. Montgomery,[13,14] T. K. Watson,[15] P. A. Bradley,[16] D. J. Sullivan,[17] K. Wu,[18] T. M. K. Marar,[19] S. Seetha,[19] B. N. Ashoka,[19] H. S. Mahra,[19] B. C. Bhat,[19] V. C. Babu,[19] E. M. Leibowitz,[20] S. Hemar,[20] P. Ibbetson,[20] E. Mashals,[20] E. Meištas,[21][‡] P. Moskalik,[22] S. Zoła,[23,24] J. Krzesiński[24] and G. Pajdosz[24]

[1]*Department of Astronomy, University of Cape Town, Rondebosch 7700, South Africa*
[2]*South African Astronomical Observatory, PO Box 9, Observatory 7935, South Africa*
[3]*MR, Nordlysobservatoriet, Universitetet i Tromso, N-9037 Tromso, Norway*
[4]*University of Oslo, Institute of Theoretical Astrophysics, PO Box 1029 – Blindern, N-0315 Oslo, Norway*
[5]*Observatoire Midi-Pyrenees, 14 Avenue E. Belin, 31400 Toulouse, France*
[6]*Instituto de Fisica, Universidade Federal do Rio Grande do Sul, 91500-970 Porto Alegre RS, Brazil*
[7]*Dep. de Fisica – UFSC, Campus Universitario – Trindade, CEP 88040-900 – Florianopolis SC, Brazil*
[8]*Sharp Laboratory, Department of Physics and Astronomy, University of Delaware, Newark, DE 19716, USA*
[9]*Department of Physics and Space Sciences, Florida Institute of Technology, 150 W. University Blvd, Melbourne, FL 32901-6975, USA*
[10]*Campus Box 3255, 264 Phillips Hall, Chapel Hill, NC 27599, USA*
[11]*Iowa State University, Department of Physics and Astronomy, Ames, IA 50011, USA*
[12]*Department of Physics, Grinnell College, PO Box 805, Grinnell, IA 50112-0806, USA*
[13]*Astronomy Department, University of Texas at Austin, Austin, TX 78712, USA*
[14]*Institute for Astronomy, Türkenschanzstraße 17, A-1180 Vienna, Austria*
[15]*Information Technology Services, Southwestern University, Georgetown, TX 78626, USA*
[16]*XTA, MS B220, Los Alamos National Laboratory, Los Alamos, NM 874545, USA*
[17]*Department of Physics, Victoria University of Wellington, PO Box 600, Wellington, New Zealand*
[18]*Research Centre for Theoretical Astrophysics, School of Physics, University of Sydney, NSW 2006, Australia*
[19]*Technical Physics Divison, ISRO Satellite Centre, Airport Road, Bangalore 560 017, India*
[20]*University of Tel Aviv, Department of Physics and Astronomy, Ramat Aviv, Tel Aviv 69978, Israel*
[21]*Institute of Theoretical Physics and Astronomy, Goštauto 12, Vilnius 2600, Lithuania*
[22]*Copernicus Astronomical Center, Polish Academy of Sciences, ul. Bartycka 18, 00-716 Warsaw, Poland*
[23]*Astronomical Observatory, Jagiellonian University, ul. Orla 171, 30-244 Cracow, Poland*
[24]*Mt Suhora Observatory, Cracow Pedagogical University, ul. Podchorazych 2, 30-084 Cracow, Poland*

ABSTRACT

We present a detailed mode identification performed on the 1994 Whole Earth Telescope (WET) run on GD 358. The results are compared with that obtained for the same star from the 1990 WET data. The two temporal spectra show very few qualitative differences, although amplitude changes are seen in most modes, including the disappearance of the mode identified as $k = 14$ in the 1990 data. The excellent coverage and signal-to-noise ratio obtained during the 1994 run lead to the secure identification of combination frequencies up to fourth order, i.e. peaks that are sums or differences of up to four parent frequencies, including a virtually complete set of second-order frequencies, as expected from harmonic distortion. We show how the third-order frequencies are expected to affect the triplet

---

[*] Present address: Eterpy 49, 1020 Renens, Switzerland.

[†] E-mail: francois.vuille@oenocap.ch

[‡] Guest observer at Assey-Turgen Observatory, Kazakhstan.

[§] Visiting astronomer at the Laboratorio Nacional de Astrofisica/CNPq, Brazil.

[¶] Guest observer at Siding Spring Observatory, Australia.

structure of the normal modes by back-interacting with them. Finally, a search for $\ell = 2$ modes was unsuccessful, not verifying the suspicion that such modes had been uncovered in the 1990 data set.

Key words: stars: individual: GD 358 – stars: variables: other – white dwarfs.

1 INTRODUCTION

Variable white dwarfs are believed to pulsate in non-radial gravity modes, or g-modes (Warner & Robinson 1972; Dolez & Vauclair 1981; Winget & Fontaine 1982; Kepler 1984). Their multiperiodicity requires very long continuous data in order for their period structure to be resolved, for which purpose the Whole Earth Telescope (WET; Nather et al. 1990) has been designed. Any pulsation mode can be represented by a solution of the differential equations describing stellar pulsations, of the form (e.g. Unno et al. 1989)

$$\zeta(r, \theta, \varphi, t) = \xi_k(r) Y_\ell^m(\theta, \varphi) \, e^{-i\sigma t},$$

where $\zeta(r, \theta, \varphi, t)$ describes the displacement from equilibrium of any point in the star with spherical coordinates (r, θ, φ). $\xi_k(r)$ is the radial eigenfunction, with k nodes between the centre and the surface, which describes the radial behaviour of the star. $Y_\ell^m(\theta, \varphi)$ is the spherical harmonic function of index ℓ and m ($\ell = 0, 1, 2, \ldots; m = 0, \pm 1, \ldots, \pm \ell$), while $\sigma = \sigma_{k\ell m}$ is the oscillation frequency. The ℓ and m indices describe the angular behaviour of the oscillations, which can be visualized on the surface of the star as alternate bright and dim areas. For a given stellar model, a normal mode is entirely determined by the three indices (k, ℓ, m).

Mode identification, that is the labelling of each frequency present in the temporal spectrum with its corresponding set of indices (k, ℓ, m), is the essential link between theory and observation. Asteroseismology uses the pulsations in order to extract physical information about the star, by providing the input parameters to the theoretical models (Winget 1988; Kawaler & Hansen 1989), and can only be performed once correct mode identification has been carried out. Unfortunately, mode identification is not at all a straightforward exercise, for various reasons.

(i) To the limit of a typical frequency resolution, various (k, ℓ, m) combinations can often match a given observed period.

(ii) Only the modes having an amplitude significantly above the noise level can be detected and possibly identified.

(iii) Modes with spherical order $\ell \geq 4$ are not expected to be visible photometrically, because the light received in the telescopes is unavoidably integrated over the stellar disc, and the numerous bright and dim areas on the stellar surface geometrically tend to cancel each other out (Dziembowski 1977).

(iv) The frequencies of the normal modes depend on various structural parameters of the star, which are a priori not accurately known.

(v) The observed periods do not necessarily correspond to normal modes. Harmonics and combination frequencies caused by pulse shape effects are often present (Brickhill 1992; Brassard et al. 1995; Vuille & Brassard 2000a).

(vi) Artefact frequencies, called aliases, may appear in the period spectrum because of gaps in the data set (Scargle 1981, 1982; Nather et al. 1990).

(vii) Not all successive overtones are excited. For reasons not clearly understood, the mode selection mechanism tends to excite a few frequencies among all the possible ones (Winget & Fontaine 1982).

(viii) The process of mode trapping, caused by the steep composition changes in the white dwarf interiors, may slightly shift the natural frequencies of the normal modes. The oscillation periods may thus deviate from their asymptotic equal spacing (e.g. Brassard et al. 1992).

GD 358 was the first DB pulsator to be discovered (Winget et al. 1982). It has since been observed twice with the WET, in 1990 and 1994 respectively. The very good coverage and signal-to-noise ratio obtained during the 1990 WET run led to quite a secure mode identification that labelled all the normal modes with a spherical index of $\ell = 1$ (Winget et al. 1994). Mode identification performed on the 1994 WET data is reported here, and a detailed comparison with the 1990 results is carried out. A comparison of the seismological model that best fits the new data with the models of Bradley & Winget (1994), which fitted the 1990 period spectrum, will be reported elsewhere (Bradley, in preparation).

The rest of our paper is organized as follows. Section 2 presents the 1994 WET data; Section 3 reports the complete mode identification, and discusses the differences from the 1990 results; Section 4 concludes the analysis.
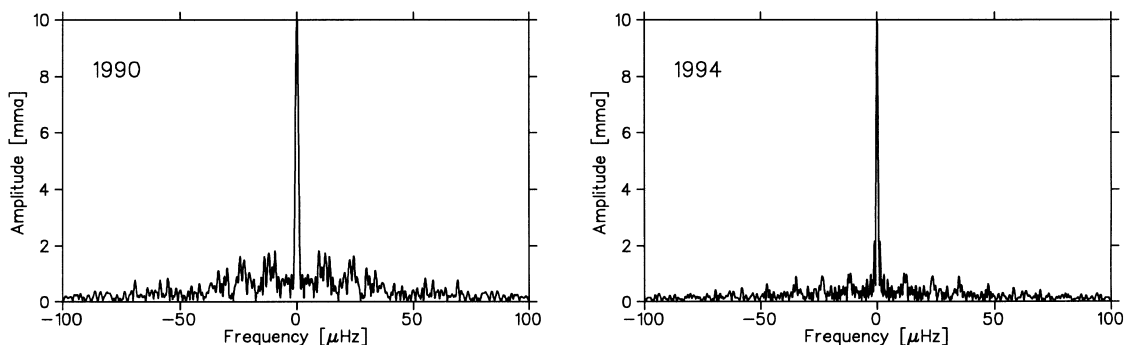

Figure 1. Comparison of the spectral windows as observed in 1990 (left panel) and 1994 (right panel).

Table 1. Journal of observations.

Telescope	Run name	Date (UT)	Start time (UTC)	Run length (s)
Mauna Kea 0.6-m	jcc-0225	1994 May 2	11:56:00	10500
Sid. Spring 0.6-m	sjk-0322	1994 May 2	14:29:30	18890
OHP 1.9-m	gv-0404	1994 May 2	22:35:10	15430
NOT[1] 2.5-m	jesb01	1994 May 3	1:08:10	15950
McDonald 0.75-m	ra321	1994 May 3	4:33:50	23830
Mauna Kea 0.6-m	jcc-0226	1994 May 3	7:54:00	1470
Mauna Kea 0.6-m	jcc-0227	1994 May 3	8:20:00	22920
Sid. Spring 0.6-m	sjk-0323	1994 May 3	16:07:30	12860
OHP 1.9-m	gv-0406	1994 May 3	21:06:00	20680
NOT 2.5-m	jesb03	1994 May 3	21:46:40	2610
SAAO 0.75-m	sa-b004	1994 May 3	22:13:10	11610
McDonald 0.9-m	ra322	1994 May 4	3:20:20	450
McDonald 0.9-m	ra323	1994 May 4	3:38:30	20860
Mauna Kea 0.6-m	jcc-0229	1994 May 4	7:40:00	25300
Sid. Spring 0.6-m	sjk-0327	1994 May 4	13:26:00	12530
Sid. Spring 0.6-m	sjk-0328	1994 May 4	16:55:30	9710
SAAO 0.75-m	sa-b009	1994 May 4	21:27:00	13060
NOT 2.5-m	jesb08	1994 May 4	21:46:00	27920
Mt. Suhora 0.6-m	suh-0007	1994 May 4	22:00:00	10530
SAAO 0.75-m	sa-b010	1994 May 5	2:34:30	5260
McDonald 0.9-m	ra325	1994 May 5	3:09:50	27010
Mauna Kea 0.6-m	jcc-0231	1994 May 5	7:36:00	25040
Sid. Spring 0.6-m	sjk-0332	1994 May 5	13:02:00	14770
Sid. Spring 0.6-m	sjk-0333	1994 May 5	17:15:00	1940
Nainital 1-m	n44-0254	1994 May 5	17:27:10	12620
OHP 1.9-m	gv-0408	1994 May 5	21:10:20	20460
NOT 2.5-m	jesb09	1994 May 5	21:20:40	29450
SAAO 0.75-m	sa-b013	1994 May 5	21:53:20	12320
McDonald 2.1-m	ra326	1994 May 6	6:09:00	13690
Mauna Kea 0.6-m	jcc-0233	1994 May 6	8:54:00	20200
McDonald 0.9-m	ra328	1994 May 6	10:57:00	970
Sid. Spring 0.6-m	sjk-0337	1994 May 6	12:54:00	22580
OHP 1.9-m	gv-0410	1994 May 6	20:36:30	22370
SAAO 0.75-m	sa-b015	1994 May 6	21:31:40	9570
Itajuba 1.6-m	ro050	1994 May 7	4:38:50	13450
Mauna Kea 0.6-m	jcc-0235	1994 May 7	7:32:00	24780
Sid. Spring 0.6-m	sjk-0341	1994 May 7	12:48:30	22600
Nainital 1-m	n44-0255	1994 May 7	15:47:10	25430
OHP 1.9-m	gv-0412	1994 May 7	20:54:20	10180
SAAO 0.75-m	sa-b017	1994 May 7	21:54:20	22070
Itajuba 1.6-m	ro051	1994 May 8	2:59:20	10100
Mauna Kea 0.6-m	jcc-0237	1994 May 8	7:26:00	25420
Sid. Spring 0.6-m	sjk-0345	1994 May 8	12:46:00	22620
Mt. Suhora 0.6-m	suh-0008	1994 May 8	20:13:30	19860
Wise 1-m	el-005	1994 May 8	20:15:41	240
Wise 1-m	el-006	1994 May 8	20:19:44	560
Wise 1-m	el-007	1994 May 8	20:54:01	9230
SAAO 0.75-m	sa-b020	1994 May 8	22:06:50	20270
Wise 1-m	el-008	1994 May 8	23:41:51	7500
Mauna Kea 0.6-m	jcc-0238	1994 May 9	10:23:00	14680
Sid. Spring 0.6-m	sjk-0349	1994 May 9	12:47:00	22590
Wise 1-m	el-010	1994 May 9	14:59:58	3206
OHP 1.9-m	gv-0414	1994 May 9	21:16:50	19390
SAAO 0.75-m	sa-b022	1994 May 9	21:23:40	21870
Itajuba 1.6-m	ro056	1994 May 10	6:46:50	3880
Mauna Kea 0.6-m	jcc-0240	1994 May 10	7:15:00	11550
Mauna Kea 0.6-m	jcc-0241	1994 May 10	10:33:40	14800
Sid. Spring 0.6-m	sjk-0350	1994 May 10	12:38:30	19240
Nainital 1-m	n44-0256	1994 May 10	15:21:10	26750
Sid. Spring 0.6-m	sjk-0351	1994 May 10	18:02:00	3340
Wise 1-m	el-011	1994 May 10	18:35:22	230
Wise 1-m	el-012	1994 May 10	19:15:51	200
Wise 1-m	el-013	1994 May 10	19:27:50	2340
Wise 1-m	el-014	1994 May 10	20:17:21	19520
Mt. Suhora 0.6-m	suh-0009	1994 May 10	21:32:20	14760
SAAO 0.75-m	sa-5726	1994 May 10	21:42:00	20270
Itajuba 1.6-m	ro059	1994 May 11	2:24:40	1780
Itajuba 1.6-m	ro060	1994 May 11	4:01:50	1880
McDonald 2.1-m	ra332	1994 May 11	5:02:00	8750

Table 1 – *continued*

Telescope	Run name	Date (UT)	Start time (UTC)	Run length (s)
Mauna Kea 0.6-m	maw-0132	1994 May 11	7:17:20	26050
Sid. Spring 0.6-m	sjk-0352	1994 May 11	12:34:00	22580
SAAO 0.75-m	sa-5728	1994 May 11	20:53:00	23490
Mt. Suhora 0.6-m	suh-0010	1994 May 11	21:58:30	11970
McDonald 2.1-m	ra333	1994 May 12	3:19:50	2640
Mauna Kea 0.6-m	maw-0134	1994 May 12	7:15:00	26200
Mt. Suhora 0.6-m	suh-0011	1994 May 12	20:29:30	17020
SAAO 0.75-m	sa-5730	1994 May 12	20:42:00	24100
Mauna Kea 0.6-m	maw-0136	1994 May 13	7:02:10	3590
McDonald 2.1-m	tkw-0045	1994 May 13	9:00:30	7310
Mauna Kea 0.6-m	maw-0137	1994 May 13	9:19:10	4460
Mauna Kea 0.6-m	maw-0138	1994 May 13	11:30:50	10690
Sid. Spring 0.6-m	sjk-0358	1994 May 13	12:42:30	21520
Mt. Suhora 0.6-m	suh-0012	1994 May 13	19:50:20	21120
McDonald 2.1-m	tkw-0046	1994 May 14	4:14:00	13840
Mauna Kea 0.6-m	maw-0140	1994 May 14	7:00:00	26900
Sid. Spring 0.6-m	sjk-0362	1994 May 14	12:47:00	21010
McDonald 2.1-m	tkw-0047	1994 May 15	5:29:30	19890
Mauna Kea 0.6-m	maw-0142	1994 May 15	6:56:20	27040
Sid. Spring 0.6-m	sjk-0367	1994 May 15	12:31:30	21660
Mt. Suhora 0.6-m	suh-0013	1994 May 15	20:49:10	16880
McDonald 2.1-m	tkw-0049	1994 May 16	4:23:00	19640
Mauna Kea 0.6-m	maw-0144	1994 May 16	6:49:00	6540
Sid. Spring 0.6-m	sjk-0372	1994 May 16	12:40:00	21060

[1] Based on observations made with the Nordic Optical Telescope (NOT), operated on the island of La Palma jointly by Denmark, Finland, Iceland, Norway, and Sweden, in the Spanish Observatorio del Roque de los Muchachos of the Instituto de Astrofisica de Canarias.

2 THE 1994 WET DATA

Although the quality of the 1990 WET campaign on GD 358 was excellent (~65 per cent coverage), the 1994 one was even better, as seen for example by comparing the two corresponding spectral windows, which represent the Fourier transforms of a single sinusoidal wave sampled as the respective data sets (Fig. 1); the largest side-lobes are only about 10 per cent in amplitude, compared with nearly 20 per cent in the 1990 data set. 342 h of high-speed photometric observations were gathered over 2 weeks with a network of 10 telescopes well distributed around the world [South Africa (SAAO), La Palma (NOT), France (OHP), Brazil (Itajuba), Texas (McDonald), Hawaii (Mauna Kea), Australia (Siding Spring), India (Nainital), Israel (Wise) and Poland (Mt. Suhora)]. About 69 h of data were actually overlapping, i.e. two telescopes were simultaneously observing the star. Therefore the campaign in effect yielded 273 h of independent observations, corresponding to an unprecedented 80 per cent coverage. Observations were carried out under photometric conditions using two or three channel photometers equipped with photomultiplier detectors with bi-alkali photocathodes. Photons have been gathered in consecutive 10-s integrations, and no filter was used, in order to increase the signal-to-noise ratio.

The 93 runs (Table 1) were reduced individually by subtracting the sky background and correcting for atmospheric extinction, before being combined together into a single light curve; details can be found in Nather (1995). Fig. 2 shows a 24-h portion of the concatenated light curve, where the coverage is best. It can be seen that the signal-to-noise ratio is extremely high, which should allow us to identify even more peaks than in 1990.
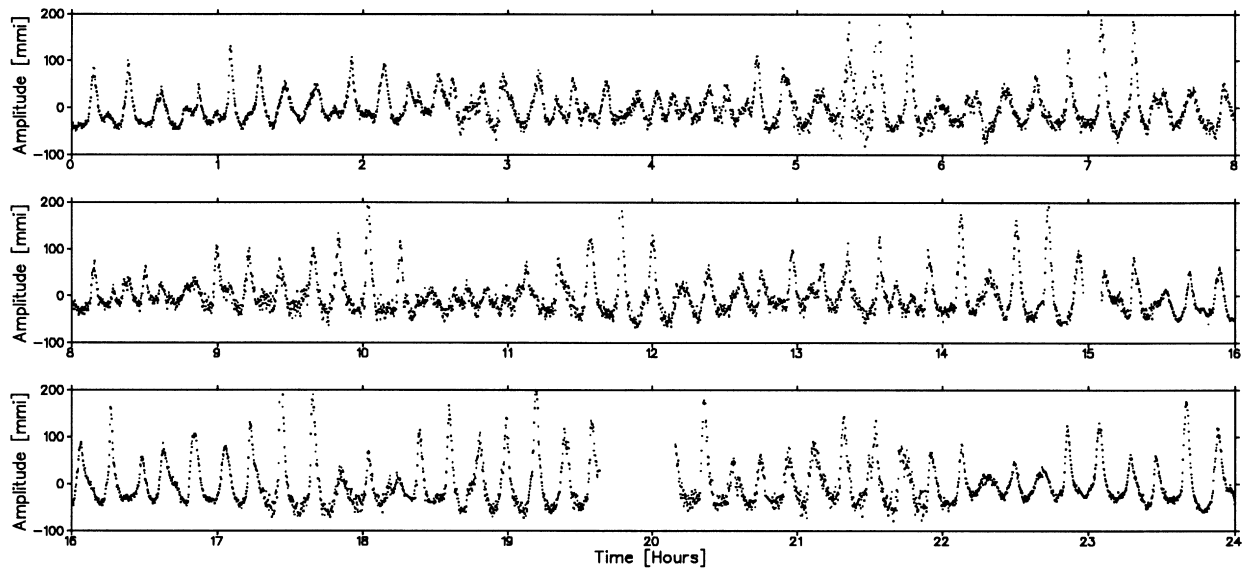
Figure 2. A 24-h portion of the light curve of GD 358 as obtained during the 1994 WET campaign, after the individual runs from the different telescopes have been combined together. Only two small gaps are apparent.
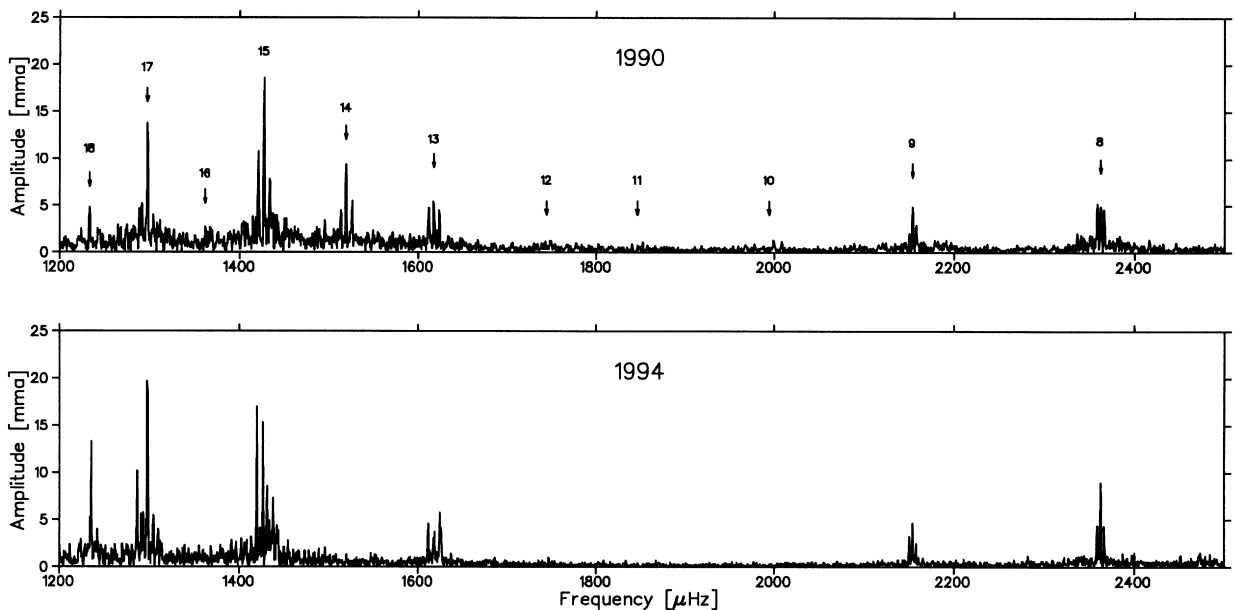

Figure 3. Comparison of the temporal spectra, in the frequency interval with largest amplitude, from the 1990 (upper panel) and 1994 (lower panel) WET campaigns. The radial orders k identified in the 1990 spectrum are indicated in the top panel.

3 MODE IDENTIFICATION

3.1 Comparison with the 1990 spectrum

The present mode identification is based on the analysis carried out on the 1990 WET data (Winget et al. 1994), as well as on the progress report by Nather (1995), which pointed out the qualitative resemblance between the 1990 and 1994 period spectra. Based on the above analyses, most 1994 multiplets found in the range 1200–2500 μHz can readily be identified as the ones observed in 1990 (Fig. 3).

While the two spectra look quite similar at first glance, there are significant quantitative differences between them. Most importantly, nearly all the modes experienced significant amplitude changes. The mode $k = 14$, third largest mode in 1990, almost disappeared in our data set. A closer look shows that the central peak of this triplet can still be found, although it is barely above the noise level, making its identification somewhat less certain. The $k = 18$, $k = 17$, and $k = 8$ modes experienced significant growth, while the $k = 11$ and $k = 10$ modes became undetectable. These last two modes were only marginally detectable in the 1990 data set.

3.2 The 'odd' multiplet structures

Although the labelling of each multiplet in this data set with its k-order was a straightforward exercise, thanks to the work of
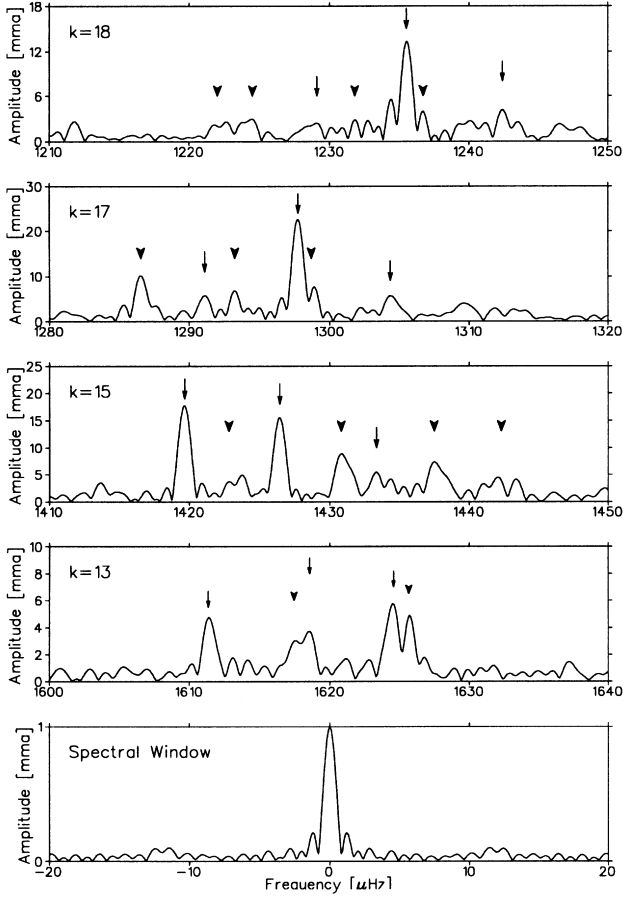
Figure 4. Close-up on the four multiplets that dominate the period spectrum. In each case, the frequencies that are thought to form the original triplets are marked with arrows, while the extra significant 'odd' peaks, those not removed by the pre-whitening procedure, are indicated by arrowheads. The bottom panel shows the corresponding spectral window.

Winget et al. (1994), the identification of each of their individual m-components requires a closer analysis. This is because the regular triplet structures recorded in 1990 do not repeat as obviously in 1994 (Fig. 3). In particular, this is the case for the four dominant modes, namely $k = 18$, 17, 15 and 13, each of which displays a complicated pattern of peaks. Fig. 4 is a close-up of these four multiplets, where the frequencies that are probably part of the triplet identified in the 1990 data are marked with long arrows, while the extra significant 'odd peaks' are indicated by arrowheads. The modes $k = 8$ and 9 do not exhibit this structure, as they both form a distinctive triplet, the components of which can be readily identified (Fig. 3).

In his progress report, Nather (1995) has shown that all the little peaks (referred to as the 'grass') surrounding the $k = 8$ triplet are caused by spectral leakage from the data gaps (Nather et al. 1990). When an artificial light curve synthesized from only the three frequencies of the triplet, and sampled as the original data, is subtracted from the observed light curve, all the small surrounding peaks are eliminated. This is, a priori, surprising as the spectral window (Fig. 1) looks impressively good. This exercise, however, shows that the combined window effect of closely separated frequencies can have a complementary effect much more significant than the spectral window might suggest.

We applied a pre-whitening procedure to try and clarify the situation for the $k = 18$, 17, 15 and 13 multiplets. In order to
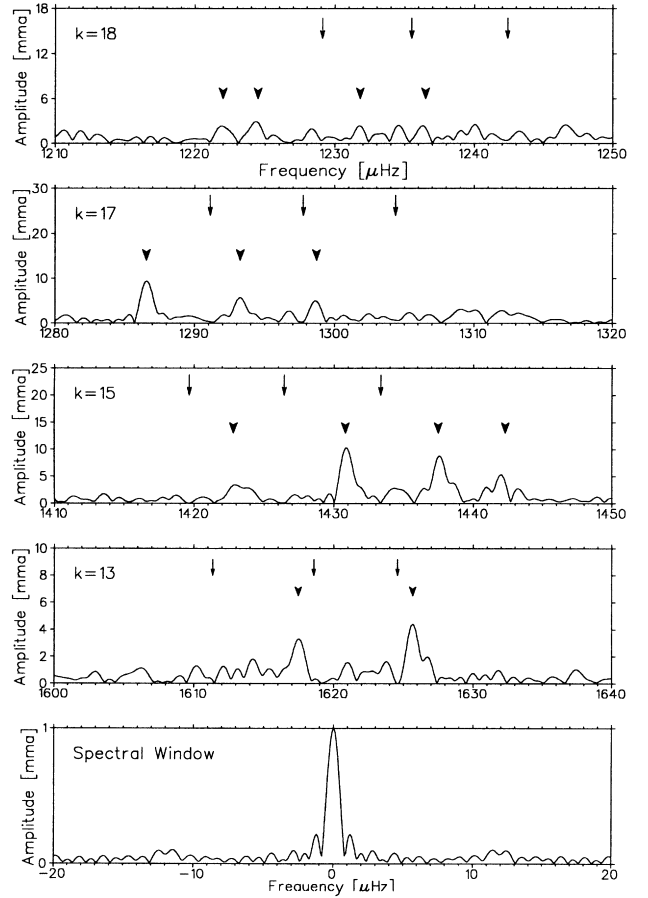
Figure 5. Replot of Fig. 4, where the peaks that were marked with arrows have been simultaneously fitted by non-linear least-squares fits and removed. Their positions are still indicated by arrows, while the dominant remaining 'odd' peaks are again marked by arrowheads.

differentiate between real modes and possible window artefacts, the larger peaks were successively removed, in each of the above multiplets, by the traditional pre-whitening technique. This means that a synthetic light curve was constructed using the frequency, amplitude, and phase obtained by non-linear least-squares fitting the highest peak of a given multiplet. This synthetic sinusoid was then subtracted from the original light curve, and the resulting Fourier spectrum was then recomputed. This whole procedure was then repeated with the next highest peak, until no significant power was left. Very simply stated, the peaks that had to be removed by this pre-whitening technique, i.e. all the ones marked with arrows and arrowheads in Fig. 4, are probably real, while the ones that disappeared naturally during the process are probable window artefacts. This procedure does assume the absence of amplitude modulation on time-scales significantly shorter than the WET run; any amplitude variation present would also leave behind some small peaks that are spurious.

This procedure did indeed 'mow the lawn', as noticed by Nather (1995) for the $k = 8$ multiplet, in the sense that all the small peaks around each of the multiplets considered were satisfactorily removed. This however did not affect any of the 'odd' large amplitude peaks, the ones indicated by arrowheads in Fig. 4, and no simple triplet structure could thus be uncovered. A simultaneous removal of the peaks marked with arrows in Fig. 4, which is the technique actually used by Nather (1995), did not remove any of the peaks marked by arrowheads either, as seen in Fig. 5.

We then realized that all these 'odd' frequencies are situated at between 11 and 12 μHz from the peaks of the triplets identified in 1990. This suggests that they could be diurnal aliases, repeating with a frequency of 11.6 μHz (which corresponds to a 24-h period). We first considered a possible timing error, where the clock of one of the observing sites might not be properly synchronized with the others. A synthetic light curve of the length of the entire campaign was built from the 33 largest frequencies securely identified in the temporal spectrum. We then computed cross-correlation functions between each individual run and the corresponding portion of this synthetic light curve. The purpose of this procedure was to determine whether one of the observing sites might show a shift in all of its runs compared with the mean of all the timings, as represented in the synthetic light curve. No timing error was, however, uncovered, to the ~10 s resolution given by this method.

Various other attempts to try to uncover the origin of these 'odd' side peaks (Fig. 4) were unsuccessful. For instance, we investigated the possibility of frequency, amplitude or phase variations of the normal modes during the course of the observing campaign. Such changes would introduce potentially asymmetrical side lobes around the varying frequencies.

The case of the 1:1:1 resonance, mode coupling process occurring between the components of each triplet, may produce amplitude modulation, periodic or chaotic, under the condition that the prograde and retrograde frequency splittings of the triplets be uneven (Buchler, Goupil & Serre 1995). Unequal splittings are indeed observed in GD 358 (see Section 3.4), but we nevertheless believe that such resonances cannot account for the observed 'odd' frequencies, although no argument can strictly discard this process. A strong non-periodic modulation of both the phase and the amplitude of the components of each triplet would be necessary to produce the observed asymmetric 'odd' peak distribution. Such complicated resonant processes are possible, but somehow unlikely. Furthermore, no evidence of such resonance was present in the 1990 data set, and it is hard to believe that, all of a sudden, each eigentriplet finds itself individually involved in such a coupling process.

We were led to the conclusion that all the peaks marked out in Fig. 4 are real, in the sense that they are of genuine stellar origin, rather than being artefacts of the observing and/or time series analysis techniques. Also, these cannot be a simple superposition of $\ell = 1$ and $\ell = 2$, or 3, multiplets, because the period spacing between successive modes (multiplets) is not the same for different ℓ (Kawaler, Hansen & Winget 1986; see also Section 3.5).

3.3 A probable origin of the 'odd' multiplet structures

Consider the simple case of a star pulsating in two eigenmodes with frequencies ν and μ respectively. If the star is a low-amplitude pulsator, only two (first-order) peaks will appear in the period spectrum, at frequencies ν and μ. If the two modes have a high enough amplitude, non-linear pulse shape distortion might become important enough that higher order peaks will become visible in the spectrum, in the form of harmonics and combination frequencies (Brickhill 1992; Brassard et al. 1995; Wu 1998). To the second order of perturbation, peaks will be found at frequencies 2ν, 2μ, $\nu + \mu$ and $|\nu - \mu|$. To the third order, 10 new combinations can appear, at frequencies 3ν, 3μ, $2\nu + \mu$, $\nu + 2\mu$, $|2\nu - \mu|$, $|\nu - 2\mu|$, $2\nu - \nu$, $2\mu - \mu$, $\nu + \mu - \mu$ and $\nu + \mu - \nu$, that will naturally start to back-interact with the normal modes. Indeed, the original eigenmode at ν (resp. μ) has extra

power added to it in the form of the third-order components $2\nu - \nu$ and $\nu + \mu - \mu$ (resp. $2\mu - \mu$ and $\nu + \mu - \nu$).

From the third order of perturbation upwards, the notion of normal modes being simple peaks does not exist any more, as the non-linear frequencies generated by the finite-amplitude eigenmodes back-interact with the latter, resulting in each peak in the spectrum becoming a complex set of components. The story becomes even more intricate in the case where ν and μ are both split by stellar rotation (Unno et al. 1989) into a triplet with components (ν_-, ν_0, ν_+) and (μ_-, μ_0, μ_+). For instance, the resulting central peak at frequency ν_0 will be a superposition of 12 components generated as follows:

$$\nu_0,$$

$$2\nu_0 - \nu_0, \qquad \nu_0 + \nu_- - \nu_-, \quad \nu_0 + \nu_+ - \nu_+,$$

$$\nu_0 + \mu_- - \mu_-, \quad \nu_0 + \mu_0 - \mu_0, \quad \nu_0 + \mu_+ - \mu_+,$$

$$\nu_- + \nu_+ - \nu_0, \quad \nu_- + \mu_+ - \mu_0, \quad \nu_- + \mu_0 - \mu_+,$$

$$\nu_+ + \mu_- - \mu_0, \quad \nu_+ + \mu_0 - \mu_+.$$

In the presence of a magnetic field or differential rotation, as may be the case for GD 358 (Winget et al. 1994), the frequency splitting is not constant any more, but becomes dependent on both k and m (Jones et al. 1989). In this case, the above five last components would not fall exactly at the original eigenfrequency ν_0. This clearly indicates how a simple triplet structure can potentially be altered by third-order combination peaks when harmonic distortion is strong enough. This principle, proposed by Brassard (private communication), has been conceptually illustrated here with two triplets only. It is nevertheless not difficult to extrapolate what can be expected in the case of a real star with numerous modes excited.

The multitude of third-order combination frequencies identified in the temporal spectrum of GD 358 (see Section 3.4) provides ample evidence that such harmonic distortion is present. We can thus try to apply this principle to its six large-amplitude normal modes, each of which displays a triplet structure. It is easy to show that each triplet generates, on its own, 18 back-interacting third-order frequencies, while the combination with any other triplet creates 27 third-order components in each triplet. This implies that each triplet in GD 358 is, to third order of perturbation, made of $18 + (6 - 1) \times 27 = 153$ components. Even if tiny as individuals, these components are so numerous that they can have large enough combined amplitudes to transform a simple triplet into a

Table 2. Blending of the triplets $k = 16$, 15 and 13 by accidental third-order matches. The first and second columns indicate the k-order of the eigentriplets and the frequency of their central peak. The third column indicates which non-linear frequencies, described by the k-order of the modes that combine to form them, accidentally blend the eigentriplets listed in the first column. The last column shows where these non-linear frequencies fall, and should be compared with column 2.

k	ν_k (μHz)	$k_1 + k_2 - k_3$	$\nu_1 + \nu_2 - \nu_3$ (μHz)
16	1362.468	$2 \times 17 - 18$	1364.206
16	1362.468	$18 + 15 - 17$	1359.923
15	1426.402	$18 + 13 - 15$	1433.687
13	1617.502	$2 \times 15 - 18$	1617.273

rich complex multiplet. All that is needed is a significant third-order effect, which is precisely the case for GD 358 (see Section 3.4).

The multiplets $k = 16$, 15 and 13 are expected to be more affected by these third-order processes than the other eigenmultiplets; indeed, in addition to the 153 above components, they are also blended with other non-linear frequencies, combinations of 3 different modes, which accidentally happen to fall within these multiplets, as shown in Table 2.

These accidental third-order components are expected to be of much greater importance than the ones discussed earlier, as a combination of different modes is always stronger than a combination involving twice the same mode (Brickhill 1992). This can be clearly observed to the first order of perturbation, where harmonics are systematically smaller than the corresponding cross-frequencies (Winget et al. 1994). It is therefore not surprising to see these three triplets very strongly affected. The most obvious case is that of $k = 13$, the amplitude of which is comparable to that expected for the non-linear peak ($2 \times 15-18$) that affects it. It is not surprising either that the $k = 16$ eigenmode cannot be identified. The lack of power at this latter frequency might be caused by destructive beating between the probable $k = 16$ and the numerous third-order peaks expected.

Although the definite presence of third-order harmonic distortion strongly suggests that this effect is responsible for the alteration of the dominant triplets (Fig. 4), no theoretical model exists to date for DB variables that could provide quantitative support to this qualitative assertion. Furthermore, we cannot find a satisfactory explanation why the triplets are not similarly altered in 1990. We have applied the same pre-whitening procedure to each of the 1990 triplets, which nearly, but not quite, removed all significant power. The peaks left were, however, not significantly enough above the noise level to be claimed real.

This difference in behaviour between 1990 and 1994 could possibly be explained by the increase in amplitude recorded in most modes (Fig. 3). Because this harmonic distortion process is perturbative, a small increase in the first-order amplitudes might generate significant increase in the third-order effects. Alternatively, the 1994 triplets might be perturbed by some photometrically invisible modes with high ℓ-index that were not present in 1990. This remains, however, speculative, until observations (*Hubble Space Telescope*, line profile, etc.) or numerical calculations are able to settle the issue.

3.4 Complete $\ell = 1$ frequency table

The full amplitude spectrum is given in Fig. 6, where each panel has a different vertical scale to accommodate the wide range of amplitudes observed. The complete list of identified $\ell = 1$ modes and combination frequencies, together with their physical parameters, is given in Tables 3 to 6. All the phases φ listed have been measured with the starting time of the run being the point of reference $t_0 = 0$, which corresponds to the Julian date JD = 244 9474.503 834. The columns labelled $\delta\nu$ represent the error in the frequency identification, as given by the non-linear least-squares fits.

Table 3 describes the normal modes. As discussed in Section 3.3, the multiplets labelled $k = 13$, 15, 17 and 18 are probable blends with peaks of third-order origin. Only the frequencies that are thought to be part of the original triplet have been listed.

The last column of Table 3 indicates the frequency difference

between the same modes identified in the 1990 and 1994 campaigns. Globally speaking, no significant frequency shifts are recorded, although slight variations occurred in all the multiplets, with the exception of the $k = 8$ and $k = 9$ modes. The stability and relatively low amplitudes of these two modes reinforces our conclusion that the other dominant modes are perturbed by third-order effects. In particular, no third-order combination involving only $k = 9$ and 8, such as ($2 \times 9 + 8$) or ($2 \times 8 + 9$), could be identified.

Our eigenmode identification also supports some of the asteroseismological results of Winget et al. (1994). In particular, the slightly larger splittings of the prograde ($m = +1$) modes compared with those of the retrograde modes ($m = -1$) (Table 3, penultimate column) suggest the presence of a weak magnetic field.

Tables 4 and 5 list the second-order frequencies, i.e. the first harmonics and combination frequencies, which are respectively the differences and sums of two frequencies of $\ell = 1$ modes. Although the sums show definite multiplet structures, as expected when combining two triplets together, only the largest component has, deliberately, been identified in each case. Surprisingly enough, it is not always the expected peak corresponding to the combination of the largest components of the parent triplets. For instance, the frequency identified at 1430.837 μHz and labelled $1\hat{5}$ (see Table 3), one of the 'odd' peaks of the $k = 15$ multiplet (Fig. 4), shows many sum frequencies, while the larger $m = 0$ component at 1426.402 μHz does not.

As six eigentriplets have been securely identified in GD 358, $6^2 = 36$ combination multiplets could possibly be found to the second order of perturbation, of which 15 correspond to difference frequencies, 6 to harmonics, and 15 to sum frequencies. Virtually all of them have been found, as 31 cross-frequencies, each corresponding to the largest peak in these combination multiplets, out of 36 possible ones have been securely identified. The ones missing may be either blended with other peaks or not sufficiently above the noise level for a secure identification to be permitted. This very strongly suggests that these non-linearities are mostly harmonic distortions, in good agreement with our claim that this process is responsible, at higher order of perturbation, for the 'odd' muddled structure of the eigenmultiplets.

The limitation of our extinction removal technique produces low signal-to-noise ratio below $\sim 200 \mu$Hz. The identification of difference frequencies in this spectral region therefore remains uncertain, and should be considered with caution.

Table 6 lists the third- and fourth-order frequencies. Although numerous third-order combinations were found in the 1990 spectrum, the very high signal-to-noise ratio of this 1994 run allowed, for the first time, the identification of fourth-order combination modes (two of them), i.e. frequencies that are the sum of four frequencies of normal modes. Note that many peaks have been identified that are combinations involving the frequency $k = 1\hat{5}$ at 1430.837 μHz in the $k = 15$ multiplet (Table 3). If this $k = 1\hat{5}$ is itself a third-order frequency, it means that the combinations in Table 6 involving this frequency are thus of the fifth or sixth order. This would be rather surprising, considering that their amplitudes are as large as those of all the other third-order combinations identified. A possibility is that the $k = 1\hat{5}$ peak is actually the $k = 15, m = +1$ mode, which has been shifted, for some unknown reason, from the position it has in the 1990 temporal spectrum. The peak at 1433.342 μHz (Table 3), instead of being the $k = 15, m = +1$ mode, could then be a third-order frequency, as discussed below.
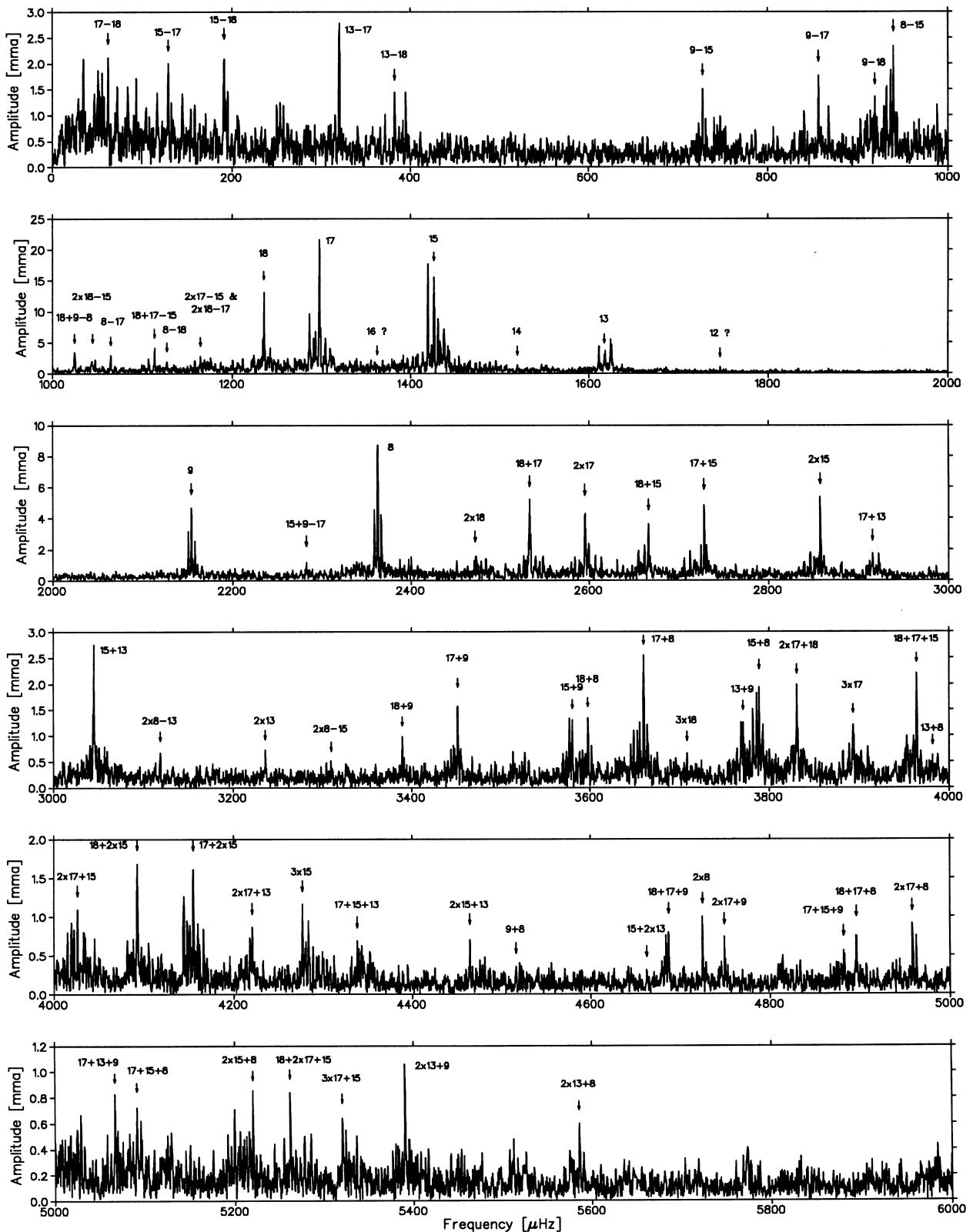
Figure 6. Complete 1994 temporal spectrum. The eigenmodes are indicated by their radial order *k*, while the cross-frequencies are labelled by the *k*-orders of the normal modes that combine to form them. The amplitude scale is given in milli-modulation amplitude (mma) units and is different for each panel.

The last column of Tables 4, 5 and 6 shows how precise the matches are between the measured frequencies of the combination modes and the calculated sums of the frequencies of the corresponding normal modes. It is quite remarkable to see that,

beside a few exceptions probably caused by blending, these matches are accurate to within a few tenths of μHz or less, i.e. barely above the frequency errors given by the non-linear least-squares fits.

Table 3. The identified $\ell = 1$ normal modes. The '?!' indicates modes that have a secure identification but that are strongly affected by the presence of peaks of probable third-order origin. The '?' indicates a less secure identification. The 'odd' peak, at 1430.837 μHz, in the $k = 15$ multiplet has been indicated because it shows many combination frequencies. It has been labelled $\hat{15}$ solely to allow reference in the discussion.

k	m	Frequency ν (μHz)	$\delta\nu$ (μHz)	Period (s)	Amplitude A (mma)	Phase φ (rad)	Splitting (μHz)	$\nu_{94} - \nu_{90}$ (μHz)
18	−1	1229.009	0.034	813.67	2.46	−1.03	6.52	–
18	0	1235.531	0.006	809.37	13.56	1.05	–	2.078
18	+1	1242.383	0.020	804.90	4.11	2.01	6.85	–
17	−1	1291.072	0.012	774.55	6.38	0.62	6.66	0.072
17	0	1297.727	0.004	770.58	22.15	2.23	–	0.147
17	+1	1304.443	0.013	766.61	6.09	−2.60	6.72	0.323
16	−1	1355.505	0.038	737.73	2.22	0.49	6.96	−0.075
16?!	0	1362.468	0.060	733.96	1.42	2.71	–	0.618
16	+1	1368.611	0.038	730.67	2.25	−0.34	6.14	0.111
15	−1	1419.626	0.004	704.41	18.63	1.93	6.78	1.644
15	0	1426.402	0.005	701.06	16.64	0.11	–	0.868
$\hat{15}$	?	1430.837	0.007	698.89	10.57	0.70	4.44	–
15	+1	1433.342	0.013	697.67	5.72	2.43	6.94	0.698
14	0	1519.960	0.064	657.91	1.32	−2.433	–	1.010
13	−1	1611.346	0.017	620.60	5.00	−2.76	7.09	−0.454
13?!	0	1618.435	0.025	617.88	3.92	−0.11	–	1.055
13	+1	1624.558	0.014	615.55	5.93	0.87	6.12	−1.062
12?	0?	1746.714	0.081	572.50	1.05	−2.70	–	2.834
9	−1	2150.490	0.027	465.01	3.14	2.61	3.64	−0.080
9	0	2154.127	0.018	464.23	4.76	0.78	–	0.027
9	+1	2157.838	0.031	463.43	2.73	−1.00	3.71	0.168
8	−1	2358.881	0.018	423.93	4.54	0.99	3.75	0.031
8	0	2362.634	0.009	423.26	9.23	2.81	–	0.074
8	+1	2366.506	0.020	422.56	4.22	−1.94	3.87	0.046

Table 4. The identified second-order difference frequencies. All are combinations of standing waves, i.e. of the $m = 0$ component of the parent modes.

Combination $k_1 - k_2$	Frequency ν_c (μHz)	$\delta\nu_c$ (μHz)	Amplitude A (mma)	Phase φ (radian)	$\nu_c - (\nu_1 \pm \nu_2)$ (μHz)
17–18	62.082	0.040	2.15	2.50	0.114
15–17	128.795	0.042	2.01	−1.62	0.120
15–18	191.012	0.038	2.24	−0.27	0.141
13–17	320.278	0.029	2.86	−2.89	0.430
13–18	382.416	0.059	1.44	−1.27	0.488
9–15	727.677	0.055	1.54	1.01	0.048
9–17	856.473	0.047	1.80	−1.53	0.073
9–18	918.772	0.062	1.36	−1.28	0.176
8–15	939.295	0.035	2.39	−0.67	3.063
8–17	1064.866	0.029	2.97	0.87	0.041
8–18	1127.118	0.043	1.98	1.64	0.015

None of the numerous third-order combination frequencies expected to blend the normal mode triplets has been identified in Table 6. The reason for this is not that we cannot identify any of them, but rather that each of the 'odd' peaks can be assigned many different identifications, because so many third-order combinations are expected to fall within a narrow frequency range. Table 7 shows possible identifications for the 'odd' peaks marked with arrowheads in Fig. 5. It appears that, with the one exception, all the observed 'odd' peaks can be identified with several third-order combinations, which strengthens our contention that these peaks are merely harmonic distortion effects.

The 'odd' peak observed at 1442.008 μHz in the triplet $k = 15$ cannot, however, be identified with any third-order frequency, even though power is definitely present there (see Fig. 5). However, if we consider the $k = 15, m = +1$ mode to be the peak labelled $k = \hat{15}$ (Table 3), instead of the peak at 1433.342 μHz, as discussed above, then the situation is quite different. Table 8 is a replot of Table 7 with this alternative identification adopted, and where the peak at 1433.342 μHz is consequently considered to be an odd frequency. The comparison of Tables 7 and 8 shows that the number of third-order combinations with which the odd peaks could be identified has increased in almost each case, and the

Table 5. The identified second-order sum frequencies. The '?!' indicates a combination with a secure k-order identification, but which is a composite blend of various m-order components of the parent multiplets. The subscripts '+' and '−' refer to the azimuthal order $m = \pm 1$, whereas no subscript means $m = 0$. The mode referred to as $\hat{1}5$ represents the 'odd' frequency at 1430.837 μHz in the $k = 15$ multiplet.

Combination $k_1 + k_2$	Frequency ν_c (μHz)	$\delta\nu_c$ (μHz)	Amplitude A (mma)	Phase φ (radian)	$\nu_c - (\nu_1 \pm \nu_2)$ (μHz)
2×18	2472.259	0.050	1.69	0.66	1.197
$18 + 17$	2533.201	0.016	5.23	2.96	0.057
2×17	2595.413	0.018	4.68	−1.83	0.041
$18 + \hat{1}5$	2666.308	0.023	3.72	1.96	0.060
$17 + \hat{1}5$	2728.535	0.017	5.04	3.11	0.029
$15 + \hat{1}5$	2857.246	0.016	5.39	0.67	0.007
$17 + 13_+$	2922.260	0.048	1.78	−2.92	0.025
$16 + 13_+$	2986.384	0.096	0.89	−0.40	0.642
$15_- + 13_+$?!	3045.225	0.031	2.76	2.81	1.041
$13_- + 13_+$	3235.984	0.120	0.73	−2.06	0.980
$18 + 9$	3389.657	0.085	0.99	1.90	0.001
$17 + 9$	3451.812	0.049	1.74	3.05	0.042
$15 + 9$	3580.477	0.064	1.32	1.10	0.052
$18 + 8$	3598.068	0.062	1.36	−2.17	0.097
$17 + 8$	3660.366	0.033	2.55	−1.25	0.005
$13 + 9$	3771.076	0.065	1.30	2.91	1.489
$15 + 8$	3788.998	0.041	2.09	−3.11	0.038
$13 + 8$	3981.578	0.140	0.63	−1.09	0.509
$9 + 8$	4516.654	0.230	0.37	−2.00	0.107
2×8	4725.263	0.084	1.01	−0.26	0.005

Table 6. The identified second- and third-order cross-frequencies. The '?!' indicates combinations with secure k-order identification, but which are intricate blends of various m-order components from the parent multiplets. The subscripts '+' and '−' indicate the azimuthal order $m = \pm 1$, whereas no subscript means $m = 0$. The mode referred to as $\hat{1}5$ represents the 'odd' frequency at 1430.837 μHz in the $k = 15$ multiplet.

Combination $k_1 + k_2 \pm k_3$	Frequency ν_c (μHz)	$\delta\nu_c$ (μHz)	Amplitude A (mma)	Phase φ (radian)	$\nu_c - (\nu_1 \pm \nu_2)$ (μHz)
$18 + 9 - 8$	1024.836	0.025	3.42	−2.28	2.188
$18 + 18_+ - \hat{1}5$	1047.691	0.038	2.24	−0.95	0.612
$18 + 17 - 15_-$	1113.524	0.020	4.18	+1.71	0.108
$2 \times 17 - 15_+$	1164.531	0.030	2.86	1.63	0.086
$15 + 9 - 17$	2282.419	0.073	1.17	−1.10	0.383
$8 + 8_+ - 13_-$	3118.864	0.130	0.68	−0.50	1.07
$8 + 8 + -15_-$	3309.679	0.162	0.53	−0.64	0.165
$18_- + 18 + 18_+$	3708.923	0.120	0.70	0.69	2.000
$2 \times 17 + 18$	3830.844	0.042	2.00	−0.14	0.141
3×17	3893.098	0.069	1.23	1.01	0.083
$18 + 17 + \hat{1}5$	3964.011	0.038	2.21	−1.96	0.084
$2 \times 17 + \hat{1}5$	4026.340	0.077	1.11	−1.05	0.049
$18 + 15 + \hat{1}5$	4092.716	0.050	1.70	2.37	0.054
$17 + 15_- + 15$	4144.509	0.065	1.30	0.17	0.754
$17 + 15 + \hat{1}5$	4155.027	0.050	1.69	2.86	0.061
$2 \times 17 + 13_+$	4220.868	0.097	0.88	0.43	0.856
$15_- + 15 + \hat{1}5$	4276.815	0.073	1.17	−3.09	0.005
$17_- + \hat{1}5 + 13$?!	4338.428	0.120	0.70	1.93	1.923
$\hat{1}5 + 15 + 13$	4464.925	0.110	0.74	−1.55	0.462
$15 + 13_- + 13_+$	4662.922	0.260	0.32	1.18	0.616
$18 + 17 + 9$	4687.374	0.097	0.88	−2.31	0.011
$2 \times 17 + 9$	4749.606	0.110	0.74	−0.57	0.025
$17 + \hat{1}5 + 9$?!	4881.714	0.140	0.59	−0.58	0.977
$18 + 17 + 8$	4895.777	0.100	0.84	0.30	0.115
$2 \times 17 + 8$	4958.048	0.092	0.92	1.20	0.040
$17 + 13_- + 9_+$	5066.454	0.100	0.84	0.89	0.457
$17 + \hat{1}5 + 8$	5090.980	0.110	0.77	0.63	0.218
$15_- + \hat{1}5 + 8$	5220.021	0.099	0.86	−2.81	0.148
$18 + 2 \times 17 + \hat{1}5$	5261.705	0.098	0.87	0.54	0.117
$3 \times 17 + 15$	5320.162	0.130	0.68	−2.24	0.579
$13_- + 13_+ + 9$	5390.458	0.079	1.07	−2.18	0.423
$2 \times 13_- + 8$	5585.843	0.140	0.62	−1.78	0.517

Table 7. Possible identifications for some of the 'odd' peaks observed within the eigentriplets. The first column indicates the triplet under concern. The second column gives the frequency of the odd peak considered. The third column indicates how many third-order frequencies are expected to fall within 1 μHz around this observed odd peak. The fourth and fifth columns indicates the best possible identification for this odd peak, while the last column shows the frequency mismatch between the observed peak and this proposed identification. The subscripts '+' and '−' refer to the azimuthal degree $m = \pm 1$, whereas no subscript means $m = 0$.

Triplet k	'odd' peak (μHz)	Possible identifications	Identification $k_1 + k_2 - k_3$	Frequency (μHz)	Mismatch (μHz)
18	1221.975	15	$18_- + 15 - 15_+$	1222.069	0.094
18	1224.413	4	$18_- + 8 - 8_+$	1225.137	0.724
18	1231.732	8	$18 + 8_- - 8$	1231.778	0.046
18	1236.412	17	$18_- + 9_+ - 9_-$	1236.357	0.055
17	1286.633	4	$17_- + 8 - 8_+$	1287.200	0.667
17	1293.331	4	$17 + 8 - 8_+$	1293.855	0.524
17	1298.578	16	$17 + 9_+ - 9_-$	1298.420	0.158
15	1422.934	8	$15 + 9_- - 9$	1422.765	0.169
15	1430.836	4	$15 + 8_+ - 8$	1430.274	0.562
15	1437.623	3	$15_+ + 8_+ - 8$	1437.214	0.409
15	1442.008	0	−	−	−
13	1617.502	20	$13_- + 13_+ - 13$	1617.469	0.033
13	1625.703	9	$13 + 9_+ - 9_-$	1625.783	0.080

Table 8. Replot of Fig. 7 where the peak labelled $k = \hat{1}5$ at 1430.837 μHz is now considered to be the $m = +1$ component of the $k = 15$ triplet, in place of the peak at 1433.342 μHz, which then becomes an 'odd' peak.

Triplet k	'odd' peak (μHz)	Possible identifications	identification $k_1 + k_2 - k_3$	Frequency (μHz)	Mismatch (μHz)
18	1221.975	15	$18_- + 15 - \hat{1}5$	1222.069	0.094
18	1224.413	6	$18 + 15_- - \hat{1}5$	1224.320	0.093
18	1231.732	10	$18 + 8_- - 8$	1231.778	0.046
18	1236.412	17	$18_- + 9_+ - 9_-$	1236.357	0.055
17	1286.633	6	$17_- + 15_- - \hat{1}5$	1286.637	0.004
17	1293.331	6	$17 + 15 - \hat{1}5$	1293.292	0.039
17	1298.578	16	$17 + 9_+ - 9_-$	1298.420	0.158
15	1422.934	14	$15 + 9_- - 9$	1422.765	0.169
15	1433.342	15	$15 + 18_+ - 18$	1433.254	0.088
15	1437.623	11	$15 + \hat{1}5 - 15_-$	1437.613	0.010
15	1442.008	1	$2 \times \hat{1}5 - 15_-$	1442.048	0.040
13	1617.502	20	$13_- + 13_+ - 13$	1617.469	0.033
13	1625.703	9	$13 + 9_+ - 9_-$	1625.783	0.080

frequency matches are more accurate. In particular, the previously unidentified peak at 1442.008 μHz can now be securely identified as the $2 \times \hat{1}5 - 15_-$ cross-frequency, both because the frequency match is excellent and because no other combination frequency is expected nearby.

Although the above results and discussion make it tempting to identify this $k = \hat{1}5$ peak with the mode $k = 15, m = +1$, it is not obvious at all that this is correct. If the latter identification is correct, it is indeed very difficult to explain the shift of this prograde mode from its 1990 position at 1434.040 μHz (Winget et al. 1994) to its 1994 position at 1430.837 μHz (Table 3), especially as no similar shift was recorded in the $m = -1$ and $m = 0$ components of this triplet, nor in any other eigentriplet.

3.5 Search for $\ell = 2$ modes

Winget et al. (1994) suggested the presence of $\ell = 2$ modes, although none could specifically be identified. This possibility encouraged them to search for a period spacing corresponding to the $\ell = 2$ range, which they found. This led them to conclude that $\ell = 2$ modes were probably present, but with amplitudes too low

above noise level for them to be identified. With the better signal-to-noise ratio of the 1994 data, we hoped that these modes could possibly be uncovered, so we repeated the search procedure. We searched for a period spacing $\Delta\Pi_\ell$ that could correspond to an $\ell = 2$ pattern in the 1994 amplitude spectrum. To do so, the period spacing for the $\ell = 1$ modes must first be determined, which then provides the typical $\ell = 2$ spacing according to the asteroseismological relation (Tassoul 1980)

$$\Delta\Pi_\ell = \frac{\Pi_0}{\sqrt{\ell(\ell+1)}} \qquad \Rightarrow \Delta\Pi_1 = \sqrt{3}\Delta\Pi_2,$$

where Π_0 is the characteristic g-mode spacing, which is a function of the stellar structure. The asymptotic period spacing $\Delta\Pi_1$ could be obtained by averaging the measured period spacings (Table 3), but the inverse variance method (O'Donoghue 1994) is a more sound statistical method for this purpose. We fitted a set of equally spaced periods to the identified $\ell = 1$ modes, and calculated the inverse variance of the residuals for each fit. The inverse variance is maximized for a period spacing of 38.9 s (Fig. 7), which we thus consider to be the $\ell = 1$ period spacing. According to the above equation, the corresponding $\ell = 2$ spacing should then be 22.5 s.
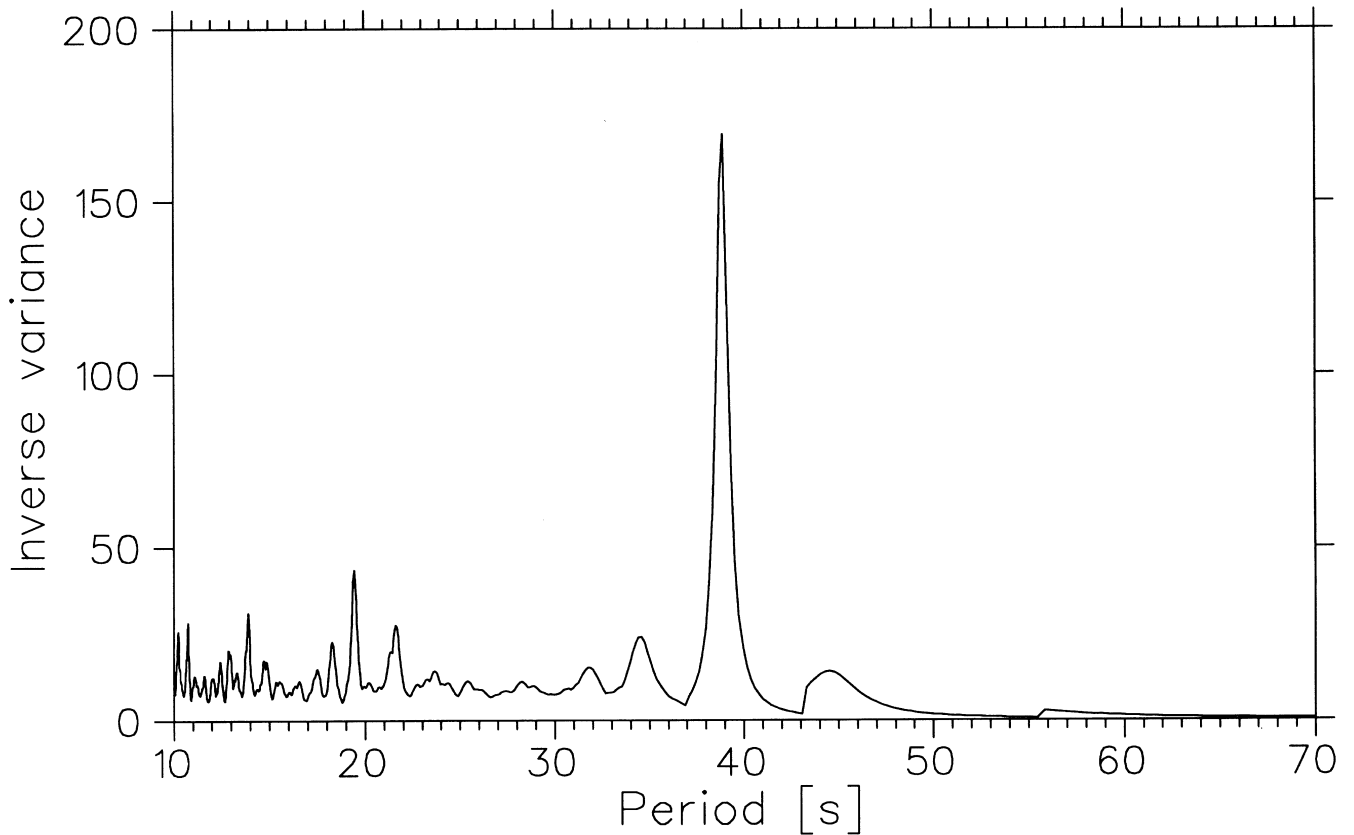
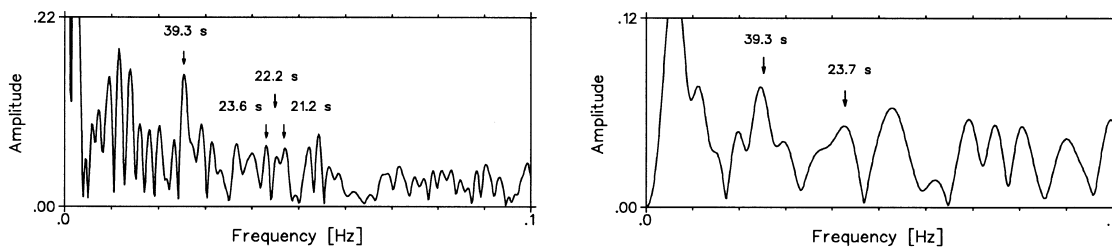**Figure 7.** Inverse variance versus period spacing.

Figure 8. Fourier transform of the period transform of the regions 1000–4000 μHz (left panel) and 2000–4000 μHz (right panel).

The inverse variance technique cannot be used to search for a possible $\ell = 2$ underlying structure, because it is a check procedure rather than a search procedure; we do not have a set of peaks that we suspect to be $\ell = 2$ modes, and we therefore have no input frequencies with which to feed the inverse variance method. A completely objective search method consists in computing the Fourier transform of the period transform (FTPT hereafter), where the latter is simply the amplitude spectrum of Fig. 6 with the frequency scale transformed into a period scale. The FTPT, computed in the range 1000–4000 μHz, is shown in the left panel of Fig. 8.

The peak at 39.3 s corresponds to the $\ell = 1$ period spacing, and is 0.4 s different from the value determined by the inverse variance method. A period spacing is found at 22.2 s, but definitely not significant enough to claim an $\ell = 2$ discovery, as it is closely flanked by two larger peaks at 21.2 and 23.6 s. An inherent difficulty is that the numerous $\ell = 1$ modes and cross-frequencies generate many period spacings, thus perturbing the search for an $\ell = 2$ spacing. Furthermore, harmonics of genuine period

spacings appear naturally in the FTPT as an obvious consequence of the computing technique.

To possibly remove all those peaks directly generated by the $\ell = 1$ multiplets, the FTPT has been recomputed in the frequency range 2000–4000 μHz, which is the range where $\ell = 2$ modes with radial order $k = 8$ to $k = 18$ should be found, according to the model by Bradley & Winget (1994). The result is shown in the right panel of Fig. 8. Not only has the peak at 21.2 s completely disappeared, but that at 22.2 s is now blended with the 23.7 s (previously 23.6 s) one, which has substantially decreased in amplitude. We would have expected the opposite behaviour, i.e. an increase in resolution and possibly amplitude, if one of these peaks were to correspond to an $\ell = 2$ period spacing.

Furthermore, it is a fairly straightforward exercise to produce a 22-s spacing using the identified cross-frequencies. For instance the sequence of modes identified as $(17 + 15)$, $(17 + 13)$, $(2 \times 8 - 13)$, $(18 + 8)$, $(18 + 17 + 15)$ and $(17 + 15 + 13)$ have the respective spacings 23.4, 22.5, 21.4, 24.3, 21.7 and 22.7 s,

averaging precisely at 22.7, which we believe contributes significantly to the peak observed in the FTPT.

For this reason, we have recomputed the FTPT shown in the right panel of Fig. 8 after having removed from the temporal spectrum, using the pre-whitening technique, all the cross-frequencies identified in the range 2000–4000 μHz (see Tables 5 and 6). The result of this exercise was no more conclusive than what can already be seen in Fig. 8. The point has to be made that this technique is limited by the fact that only the highest peak of each non-linear multiplet is removed by the pre-whitening, while each non-linear multiplet is formed from 9 peaks (because it is a combination of two eigentriplets). It is unfortunately not possible to identify securely all these 9 peaks, because of their partial blending, which limits the efficiency of this removal technique.

We conclude that, despite the better quality of the 1994 WET data, we have found no evidence for the presence of $\ell = 2$ modes in GD 358.

4 CONCLUSION

The excellent coverage and signal-to-noise ratio obtained during the 1994 WET run on GD 358 allowed us not only to confirm the mode identification carried out on the 1990 data set (Winget et al. 1994), which was the main purpose of this second campaign (Nather 1995), but also to uncover many more excited cross-frequencies. No significant peak remains in the period spectrum that has not been identified as an $\ell = 1$ eigenmode of the star or an associated cross-frequency. Although GD 358 presents a complicated spectrum, with over 70 significant peaks (Fig. 6), its underlying pulsation structure can be entirely explained in terms of just six excited eigentriplets, and the forest of distinctive combination frequencies identified.

One important question nevertheless remains regarding the identification of the prograde component of the $k = 15$ triplet. It is not clear which one of the peaks observed at 1433.342 and 1430.837 μHz (labelled $k = \hat{15}$ in Section 3.4) corresponds to this $k = 15, m = +1$ mode (see Table 3). On the one hand, the peak at 1433.342 μHz is very close to the prograde component observed in the 1990 spectrum, and the frequency splitting is consistent with that recorded in the other triplets identified. On the other hand, the peak at 1430.837 μHz is significantly larger than that at 1433.342 μHz and shows numerous combination frequencies with up to three other modes (Tables 5 and 6), whereas no combinations involving the 1433.342 μHz peak were identified. Furthermore, the 'odd' peaks blending the $k = 15$ multiplet can be readily identified as third-order cross-frequencies if $k = \hat{15}$ is considered to be the $m = +1$ component, but not so easily if we consider the 1433.342 μHz peak to be the prograde mode. The down-side of the coin when identifying $k = \hat{15}$ as the $m = +1$ triplet member is that this prograde component would have been shifted by 3.2 μHz from its 1990 position, without the $m = +1$ and $m = 0$ components having experienced a similar displacement.

The nearly complete set of second- and third-order frequencies (those missing may well be blended with other identified peaks) strongly suggests that the majority of these non-linear modes are caused by harmonic distortion, and not by other non-linear processes such as resonant mode coupling. We have conceptually shown how the third-order cross-frequencies are thought to affect the regular structure of the eigenmode triplets. However, because of the lack of a detailed theoretical model that could predict the importance of this effect for DB variables, this idea remains qualitative, although third-order frequencies are definitely present with significant amplitudes. A more detailed analysis of this non-linear phenomenon, together with an analysis of the evolution of the temporal spectrum of GD 358, will be presented in a forthcoming paper (Vuille & Brassard 2000b). The possibility that resonant mode coupling between the members of each triplet (i.e. 1:1:1 resonances) is the process responsible for the presence of these 'odd' peaks cannot be strictly discarded, although some qualitative arguments have been given against it.

The search for possible $\ell = 2$ modes remained unsuccessful, both because virtually no peaks are left unidentified in the period spectrum, and because no significant period spacing at around 22.7 s could be detected in the FTPT.

The present work, together with the corresponding paper on the 1990 WET campaign (Winget et al. 1994) provides the framework for further asteroseismological study of GD 358 and other DB variables.

ACKNOWLEDGMENTS

REFERENCES

Bradley P. A., Winget D. E., 1994, ApJ, 430, 850
Brassard P. Fontaine G., Wesemael F., Tassoul M., 1992, ApJS, 81, 747
Brassard P., Fontaine G., Wesemael F., 1995, ApJS, 96, 545
Brickhill A. J., 1992, MNRAS, 259, 529
Buchler J. R., Goupil M.-J., Serre Th., 1995, A&A, 296, 405
Dolez N., Vauclair G., 1981, A&A, 102, 375
Dziembowski W., 1977, Acta Aston., 27, 203
Jones P. W., Hansen C. J., Pesnell W. D., Kawaler S. D., 1989, ApJ, 336, 403
Kawaler S. D., Hansen C. J., 1989, in Wegner G., ed., White Dwarfs. Springer-Verlag, Berlin, p. 97
Kawaler S. D., Hansen C. J., Winget D. E., 1986, ApJ, 295, 547
Kepler S. O., 1984, ApJ, 286, 314
Nather R. E., 1995, Baltic Astron., 4, 321
Nather R. E., Winget D. E., Clemens J. C., Hansen C. J., Hine B. P., 1990, ApJ, 361, 309
O'Donoghue D., 1994, MNRAS, 270, 222
Scargle J. D., 1981, ApJS, 45, 1
Scargle J. D., 1982, ApJ, 263, 835
Tassoul M., 1980, ApJS, 43, 469
Unno W., Osaki Y., Ando H., 1989, Nonradial Oscillations of Stars, 2nd edn. Univ. Tokyo Press, Tokyo
Vuille F., Brassard P., 2000a, MNRAS, in press
Vuille F., Brassard P., 2000b, MNRAS, submitted
Warner B., Robinson E. L., 1972, Nature Phys. Sci., 239, 2
Winget D. E., 1988, in Christensen-Dalsgaard J., Frandsen S., eds, Advances in Helio- and Asteroseismology. Reidel, Dordrecht, p. 305
Winget D. E., Fontaine G., 1982, in Cox J. P., Hansen C. J., eds, Pulsations in Classical and Cataclysmic Variable Stars. Boulder Joint Institute for Laboratory Astrophysics, Boulder, p. 45
Winget D. E., Robinson E. L., Nather R. D., Fontaine G., 1982, ApJ, 262, L11
Winget D. E. et al., 1994, ApJ, 430, 839
Wu Y., 1998, PhD thesis, California Inst. Tech., Pasadena

This paper has been typeset from a T$_{\text{E}}$X/L$^{\text{A}}$T$_{\text{E}}$X file prepared by the author.